https://doi.org/10.5194/egusphere-2025-1671
Preprint. Discussion started: 15 May 2025


# Thrust moraines and rock glaciers: Relationships between subsurface structures and morphodynamics in Swiss glacier forefields dominated by glacier-permafrost interactions

Julius Kunz[1], Sebastian Buchelt[2], Tim Wiegand[1], Tobias Ullmann[2], Christof Kneisel[1]

[1]Department of Climatology, Institute of Geography and Geology, University of Wuerzburg, Wuerzburg, 97074, Germany
[2]Earth Observation Research Cluster, Institute of Geography and Geology, University of Wuerzburg, Wuerzburg, 97074, Germany

*Correspondence to*: Julius Kunz (julius.kunz@uni-wuerzburg.de)

**Abstract.** Glacier-permafrost interactions in Alpine environments significantly influence geomorphological processes, making it essential to understand the relationship between subsurface structures and surface morphodynamics for predicting landscape evolution under climate change. So far, the direct correlation between subsurface ice distribution and surface movement for thrust moraine complexes and rock glaciers remains poorly understood. This study investigates the internal structure and morphodynamics of both landform types in two Swiss glacier forefields, aiming to determine how subsurface ice content and structure influence recent surface displacements. We combined electrical resistivity tomography (ERT) with Differential Interferometric Synthetic Aperture Radar (DInSAR) to assess subsurface resistivity and surface displacement patterns. The study focuses on two sites in the Valais region (Swiss Alps), analyzing spatial movement patterns and their correlation with subsurface properties through regression analysis. ERT revealed distinct differences between the ice-rich thrust moraine complexes and the more heterogeneous internal structure of the investigated rock glaciers. DInSAR-derived displacement patterns showed that moraine complexes exhibit predominantly vertical subsidence with high seasonal variability, while rock glaciers display more consistent horizontal movement. Regression analysis confirmed strong correlations between high-resistivity zones and intense surface dynamics in moraine complexes, with the logarithm of maximum resistivity correlating with absolute horizontal displacement ($R^2 = 0.75$) and elevation change ($R^2 = 0.76$). Instead, rock glaciers exhibited weaker correlations ($R^2 \leq 0.3$), likely due to heterogeneous internal structures and more complex creep processes, which differ from the subsidence-dominated movements in the ice-rich moraines. These findings underscore the importance of distinguishing between these landform types in permafrost studies and climate change assessments.

## 1 Introduction

Glaciers and permafrost in the European Alps occur in close spatial vicinity and are both strongly affected by severe changes due to ongoing global warming in recent times. Due to higher temperatures and changed precipitation patterns, glaciers in the European Alps are shrinking (Huss et al., 2015; Sommer et al., 2020; Vincent et al., 2017), and permafrost is warming and

https://doi.org/10.5194/egusphere-2025-1671
Preprint. Discussion started: 15 May 2025


degrading in many places (Biskaborn et al., 2019; Buckel et al., 2023; Noetzli et al., 2024). These changes are accompanied by morphological processes in the corresponding areas, which can have a wide variety of consequences such as changing creep rates of rock glaciers (e.g., Fleischer et al., 2021; Kellerer-Pirklbauer et al., 2024; Marcer et al., 2019), higher frequencies of rockfall events (e.g. Hartmeyer and Otto, 2024; Pfluger et al., 2025) or thermokarst phenomena (e.g. Cusicanqui et al., 2023). Especially in areas where permafrost and glaciers have interacted in the past, high amounts of ground ice are incorporated in moraines and other glacial and periglacial landforms (Waller, 2024), which are now affected by changing climatic conditions. The last intense interactions between glaciers and permafrost took place during the glacial advance of the Little Ice Age (LIA) around 1850 CE, when especially small cirque glaciers advanced into proglacial areas partly underlain by permafrost (Haeberli, 2005; Kneisel, 2003). Most of the larger glaciers in the Alps advanced far below the local permafrost base at this time, so real interactions only took place in higher-elevated glacier forefields of smaller cirque glaciers. The often polythermal character of these smaller glaciers – especially the cold-based margins – enabled transmission of glacial stress into the proglacial area and resulted in large-scale morphological overprinting in the proglacial areas (Haeberli, 1979). During this overprinting, striking thrust moraine complexes were built up, which are also termed push moraines (e.g. Haeberli, 1979) or glacitectonized frozen landforms (e.g., Wee and Delaloye, 2022). Whereas these landforms are mainly known from polar regions (Waller et al., 2012), only few studies focus on thrust moraine complexes in alpine environments, although in mountain areas like the European Alps, these structures can be particularly large compared to the size of the advancing glacier. Thereby, not only displacement and deformation of frozen sediment took place but also a major incorporation of massive sedimentary ice (Etzelmüller and Hagen, 2005; Kneisel et al., 2000; Kunz et al., 2022; Wee and Delaloye, 2022). Both the insulating debris cover and the often very high ice content in the interior of these landforms have favoured a transition to periglacial conditions. These ensured that the structures remained comparatively stable in the subsequent retreat phase of the glaciers and changed less drastically compared to the purely glacial areas (Etzelmüller and Hagen, 2005; Harris and Murton, 2005). Nevertheless, some of these landforms also show recent surface changes and could react sensitively in the context of global warming due to their high ice content. Various studies observed the recent surface morphodynamics in many glacier forefields using in situ or remote sensing-based approaches (Cusicanqui et al., 2023; Kneisel and Kääb, 2007; Kunz et al., 2022; Wee et al., 2024; Wee and Delaloye, 2022) and confirmed some direct relationships between morphodynamics and the distribution and type of ground ice. However, more detailed information on correlations between the recent displacement rates and the existing subsurface structures as well as ice contents and ice types are still scarce.

Therefore, this study builds on a combined approach of geophysical surveying and remote-sensing-based surface displacement analysis using Differential Interferometric Synthetic Aperture Radar (DInSAR) on thrust moraine complexes and neighbouring rock glaciers in the Swiss Alps. Electrical resistivity tomography (ERT) has already demonstrated its suitability for detecting permafrost and differentiating between different types of ice in the past (Haeberli and Vonder Mühll, 1996; Hauck, 2013; Herring et al., 2023; Kneisel, 2006; Kneisel et al., 2008). Therefore, two- and three-dimensional approaches are used in this study to obtain multidimensional, larger-scale information about the internal structures of the moraines and adjacent rock glaciers. In addition, DInSAR – an increasingly common method to study alpine periglacial geomorphology and

https://doi.org/10.5194/egusphere-2025-1671
Preprint. Discussion started: 15 May 2025


morphodynamics (e.g., Bertone et al., 2022; Strozzi et al., 2020; Villarroel et al., 2022) – is used to detect surface displacement patterns and their seasonal variations at two study areas. Surface displacements were previously difficult to investigate over large areas, caused great expense and were therefore usually analyzed on smaller scales using drone flights and feature tracking (Blöthe et al., 2021; Vivero et al., 2022) or direct kinematic measurements (Cicoira et al., 2022; Kenner et al., 2017). However, the use of satellite-based SAR data now enables a higher temporal resolution and a large spatial coverage so that also seasonal changes can be explored more systematically (Buchelt et al., 2023, 2024).

The combined approach now should gain further knowledge in the recent development of high-alpine glacial-periglacial environments and should help to answer the following issues: (i) What is the current internal structure of alpine thrust moraine complexes and are there differences to neighbouring rock glaciers? (ii) What kind of surface morphodynamics takes place within the respective glacier forefields? (iii) Are there any linkages between subsurface structure and recent morphodynamics, and are there any differences in this relationship considering the different landform types?

## 2 Study sites

The investigated glacier forefields are both located in the Valais, Swiss Alps, an inner-alpine dry region, well known for the continental climate and the coexistence of glaciers and permafrost. Nevertheless, the region is characterized by strong gradients, particularly due to the pronounced relief, which is reflected in a clear regional precipitation pattern besides the normal altitudinal thermal gradient. The northern part of the Valais, where the Oberferden glacier forefield is located, shows higher precipitation than the southern part, where the Pipji glacier forefield is located (MeteoSwiss, 2023a). In the following a brief overview of the two study sites is given.

### 2.1 Pipji Glacier Forefield

The Pipji Valley (Fig. 1 a,c,e) is an eastern tributary of the Turtmann Valley at its southern terminus. The valley is surrounded by the Längi Egga crest (3079 m) in the north, and by the continuous, encircling crest on to the major north-facing walls of the Üssers Barrhorn (3610 m) in the south. The flanks of the mountain slopes and the valley floor are characterized by the former glaciation and the periglacial overprint. The Pipji Glacier created large moraine structures during its LIA advance but also in previous activities, which provided the basis for rock glacier formation in the area of the former main glacier. Due to several glacial advances and successive phases of rock glacier formation, the rock glacier consists of three different units (Units I - III, see Fig. 2a), which are characterized by different ages (Tatenhove and Dikau, 1990). Further south, towards the Barrhorn, another glacier formed a thrust moraine complex under periglacial conditions, which is situated 2650 to 2720 m a.s.l. Close by, to the west, a smaller rock glacier complex can also be found (Nyenhuis, 2005; Otto, 2006). The geology in the valley is dominated by gneiss and mica shists of the Siviez-Mischabel-Nappe in the north and by dolomites and marble in the south (Bearth, 1980). Climatic stations in the vicinity and especially at a comparable altitude are rare in the area, but Otto (2006) reported an average annual temperature of -1.2 °C in the period 2002 - 2005 in the neighbouring Hungerlitaelli at a comparable

https://doi.org/10.5194/egusphere-2025-1671
Preprint. Discussion started: 15 May 2025


altitude (2770 m) and aspect. This also matches the values provided by (MeteoSwiss, 2023a, b), which indicate a mean annual air temperature of between -1 and -2 °C and annual precipitation between 900 and 1100 mm (1991-2020) for the Pipji Valley.

### 2.2 Oberferden Glacier Forefield

The Oberferden Glacier forefield (Fig. 1 b,d,f) is located at the northwestern edge of the Lötschen Valley, northwest of the municipality of Ferden. The valley is surrounded by the summits of Schwarz- and Mauerhorn (2930 & 2943 m) in the South, the Majinghorn (3053 m) in the West as well as the Ferdenrothorn (3179 m) in the North. The climate is characterized by mean annual air temperatures between -3 and -1 °C (MeteoSwiss, 2023a) and mean annual precipitation between 1300 and 1500 mm (MeteoSwiss, 2023a). The morphology of the valley is distinctly shaped by glacial and periglacial processes and is dominated by a large thrust moraine complex in the upper part and a rock glacier in the central part (cf. Fig. 1d). The investigated moraine complex was formed north of the former Oberferden glacier at 2640 and 2810 m a.s.l. It measures about 850 m in length and about 300 m in width, and typical parallel or subparallel ridge structures characterize its surface due to glaciotectonic deformation. The rock glacier is located at the eastern and lower end of the glacier forefield between 2400 and 2580 m a.s.l. It is about 700 m long, max. 250 m wide and northeast exposed. The source of the material embedded in the rock glacier seems to be polygenetic. The orographic left side seems to be moraine-derived from a former end moraine of the Oberferden glacier. In contrast, the orographic right part appears to be talus-derived and originates from the north and northwest-exposed talus slopes between Schwarzhorn and Restigrat. Due to this, there is also a difference in substrate properties with rather medium-grained sediments on the left and rather coarse blocky material on the right half of the rock glacier.

https://doi.org/10.5194/egusphere-2025-1671
Preprint. Discussion started: 15 May 2025


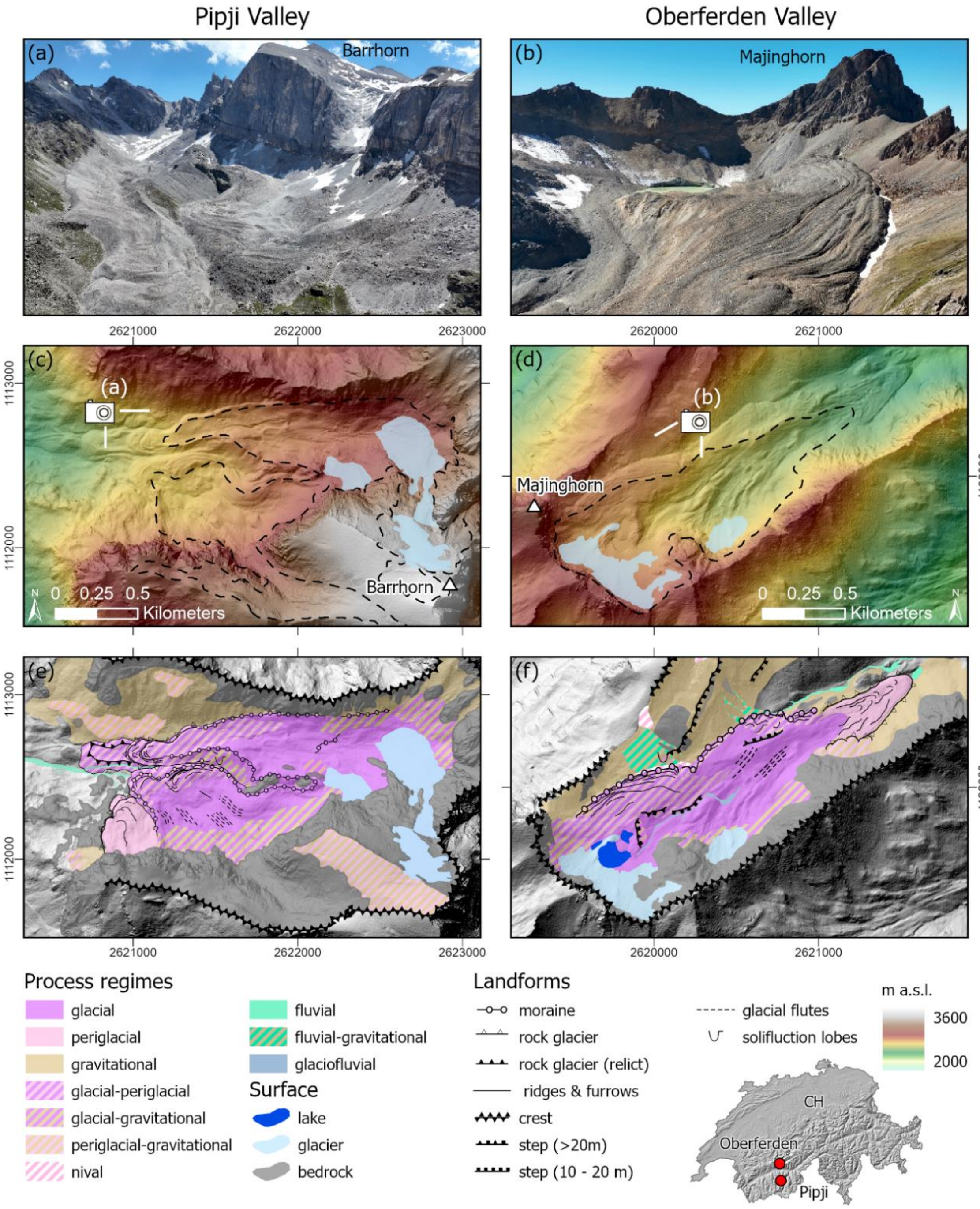


**Figure 1: Overview of the Pipji Valley (left column) and Oberferden Valley (right column). Aerial images of the study sites are shown in (a) and (b). The middle panels (c) and (d) present the relief of the study sites including the glacial extent of the Little Ice Age (1850 AD) and the image positions of (a) and (b). Geomorphological maps of the sites are shown in the lower panels (e) and (f). Mapping was conducted based on aerial images, digital elevation models and field observations in summer 2023 and 2024. Basemaps provided by © swisstopo.**

## 3 Methods and data

### 3.1 Electrical Resistivity Tomography

Electrical resistivity tomography (ERT) was used to investigate the subsurface structure within the different moraine complexes and rock glaciers. The method is common in the field of periglacial morphology and uses electrical current to determine the subsurface resistivity, which is affected by the presence of permafrost and the amount and kind of ice within the subsurface (Hauck, 2013; Herring et al., 2023; Kneisel et al., 2008). To get a comprehensive overview of the ground structure within the investigated landforms, several reconnaissance profiles were measured using a Syscal Pro Switch 72 (IRIS Instruments, Orléans, France) device, 36 electrodes, and an electrode spacing of 5 m. On both rock glaciers and the Oberferden moraine complex, a roll-along approach was conducted to cover larger areas. A quasi-three-dimensional approach comprising several parallel measurement profiles was performed at the two thrust moraine complexes to generate comparatively large multidimensional subsurface models covering areas of 175 x 120 m and 175 x 180 m. The grid positions as well as the locations of all reconnaissance profiles are shown in the respective result figures.
The subsequent data (pre-)processing included filtering by stack deviation (<5 %), incorporation of coordinates and elevation derived from DGPS and high-resolution digital elevation models, as well as an iterative inversion using the software Boundless Electrical Resistivity Tomography (BERT, v. 2.3.0.) according to Günther et al. (2006) and Rücker et al. (2006). The misfit between the generated models and the measured data is given as root-mean-square error (RMSE) for each ERT profile in the respective figure.

### 3.2 Differential Interferometry Synthetic Aperture Radar

The surface displacement in both study areas was investigated using the Differential Interferometry Synthetic Aperture Radar (DInSAR) approach developed by Buchelt et al. (2023) and C-band SAR data of the Sentinel-1 Copernicus satellite constellation (Sentinel-1 A and B). We used Single Look Complex (SLC) data in Interferometric Wide swath (IW) mode from two different orbits (relative orbit nr.: 139 - descending orbit; 088 – ascending orbit) with a temporal baseline of 6 days. The investigated period was from January 2017 to December 2021, limited by the failure of Sentinel-1B in December 2021, resulting in 298 acquisitions from descending orbit and 295 acquisitions from ascending orbit. The individual methodological steps are shortly described in the following (see Buchelt et al. 2023 for details) starting with SAR image processing in esa_snappy (python wrapper for ESA SNAP functionalities): (i) applying a recent orbit files; (ii) splitting the bursts of interest; (iii) coregistering of two consecutive SAR images; (iv) correcting for enhanced spectral diversity; (v) generation of differential interferograms with topographic phase removal using the SwissALTI3D DEM; (vi) debursting; (vii) phase filtering with a weak Goldstein Phase Filter; (viii) phase unwrapping using *snaphu* (Chen and Zebker, 2002); (ix) projection and resampling into Cartesian coordinates with a 5 m ground sampling distance. Interferograms with mean coherence below 0.5 were excluded to avoid decorrelation issues. Resulting gaps from occasional snowfall during the snow-free summer months were filled using interferograms with longer baselines (12–18 days).

https://doi.org/10.5194/egusphere-2025-1671
Preprint. Discussion started: 15 May 2025


Continuous time series stacks were then processed using pyrate (v0.5) by Geoscience Australia for additional corrections: (i) low-coherence (< 0.3) pixel masking; (ii) stable reference phase identification and subtraction; (iii) orbit error correction; (iv) atmospheric phase screen adjustments. The final output was a 6-day Line-of-Sight (LOS) displacement rate time series, used for displacement decomposition and seasonal movement analysis. Areas affected by radar shadow or layover were masked using the SwissALTI3D DEM to ensure data reliability.

For calculating annual LOS displacement, the time series was first stacked to minimize atmospheric artifacts (e.g., Rouyet et al., 2019; Sandwell and Price, 1998), then divided by the number of years covered with the time series (five) and multiplied by three in order to account for DInSAR's reduced temporal coverage, which is limited to roughly one third of the year (snow-free summer months). Displacement decomposition was then applied to convert annual LOS displacement into east-west (E-W) and up-down (U-D) components, using a simplified geometry that excluded the north-south component. However, U-D displacement reflects not just elevation changes but also slope-parallel movement on inclined slopes. To determine true elevation change, the vertical displacement was corrected for slope-induced effects using local inclination and E-W movement rates (e.g., Buchelt et al., 2024; Crippa et al., 2020; Eriksen et al., 2018). Besides, seasonal variations in movement were calculated from the 6-day LOS displacement time series, determining the absolute seasonal increase as the difference between median movement rates in June/July (early snow-free summer) and September (late snow-free summer), and relative seasonal increase as proportion of the absolute seasonal acceleration on the September velocity. A detailed description of this approach is given by Buchelt et al. (2023). The orbit with higher sensitivity in LOS was used for the respective site (Pipji: descending; Oberferden: ascending).

### 3.3 Quantitative analysis of subsurface resistivities and movement parameters

To investigate the relationship between surface movement and subsurface properties, the morphodynamical parameters of elevation change, horizontal displacement and seasonality are compared to the (apparent) resistivity values of the respective landform units, since resistivity is directly affected by the ice content and ice type. A direct derivation of ice contents is not possible without further information, but different resistivity ranges are characteristic for different permafrost properties and ice contents (Haeberli and Vonder Mühll, 1996; Kneisel, 2006). To carry out a statistical evaluation, the maximum resistivity per remote sensing pixel was determined. For this purpose, the pixel boundaries of the SAR data were transferred to the ERT profile lengths (profiles Fig. 2 c, d, Fig. 3 b, c and Fig. 4 a, b) and the maximum value over the entire depth column in the area of the respective pixel was determined. It was checked in advance that the highest values are not caused by high-resistive cells in the active layer (e.g. air-filled cavities) to ensure that the values reflect the properties of the permafrost. This confirmed that the highest values were always in deeper layers and are therefore representative. Since the wide range of the resistivity values within the individual landforms might affect a correlation, the data points were grouped depending on the maximum resistivity value in a second step. The threshold values of the groups were set based on geomorphologic-geophysical knowledge from former studies (Bosson et al., 2014; Haeberli and Vonder Mühll, 1996; Kneisel, 2006): (1) no permafrost (<10 kΩm), (2) ice-

https://doi.org/10.5194/egusphere-2025-1671
Preprint. Discussion started: 15 May 2025


poor permafrost (10 kΩm < $rho_{max}$ < 100 kΩm), (3) ice-rich permafrost (100 kΩm < $rho_{max}$ < 1 MΩm) and (4) sedimentary/massive ice (> 1 MΩm). These four classes represent the main subsurface characteristics of the glacier forefields and should be investigated separately concerning the surface morphodynamics in the respective areas.

Regression analysis was conducted using Pearson's correlation coefficient (R) to assess the linear relationships between variables. Additionally, the coefficient of determination ($R^2$), derived from squared Pearson's R, was used to evaluate the proportion of explained variance. A simple linear relationship was assumed in the absence of better knowledge on this issue, providing a first-order assessment of the association between surface displacement, resistivity, and morphometric parameters. A root-mean-square error (RMSE) was calculated to obtain a measure of the quality of the fit. In addition, a significance test was performed for each correlation, assuming a confidence level (α) of 5%. Correspondingly, significant correlations are marked with an "*" in the following.

## 4 Results and interpretation

### 4.1 Internal structure of the different landforms

In Fig. 2, a three-dimensional ERT model and a two-dimensional cross profile of the Pipji moraine complex, as well as a longitudinal profile along the neighbouring rock glacier are shown. The two-dimensional cross profile (Fig. 2 c) presents a two-layered structure of the moraine complex, with a low resistive (<15 kΩm), about 5 m thick surface-parallel upper layer and a large, high-resistive structure below. The upper layer is interpreted as the active layer, whereas the very high-resistive structure with resistivity values of up to 6 MΩm is interpreted as a massive, sedimentary ice core of the moraine complex. In the first 25 m of the profile, the high-resistive structure is missing as it represents the area outside the thrust moraine complex. Towards the end of the profile (> 130 m profile length), spanning across a thermokarst depression adjacent to the proximal flank of the moraine complex, a two-layered structure is present, but the resistivities in the deeper layer are distinctly lower than in the central part and are in a range between 40 and 50 kΩm. This structure was also confirmed by the three-dimensional ERT grid (Fig. 2 b), which covered large parts of the entire thrust moraine complex. Below the main ridge structures, resistivity values are above 1 MΩm for the entire area and reach up to more than 6 MΩm. Therefore, it is assumed that the entire complex is underlain by a massive ice core consisting of sedimentary ice. In the area of the thermokarst depression, the three-dimensional model was able to delineate the area wherein the massive ice has already melted. In the western part of the moraine complex, the presence of massive sedimentary ice was confirmed due to exposure by an active layer detachment and following thermokarst processes in summer 2024 (cf. Fig. A1 a, c).

https://doi.org/10.5194/egusphere-2025-1671
Preprint. Discussion started: 15 May 2025


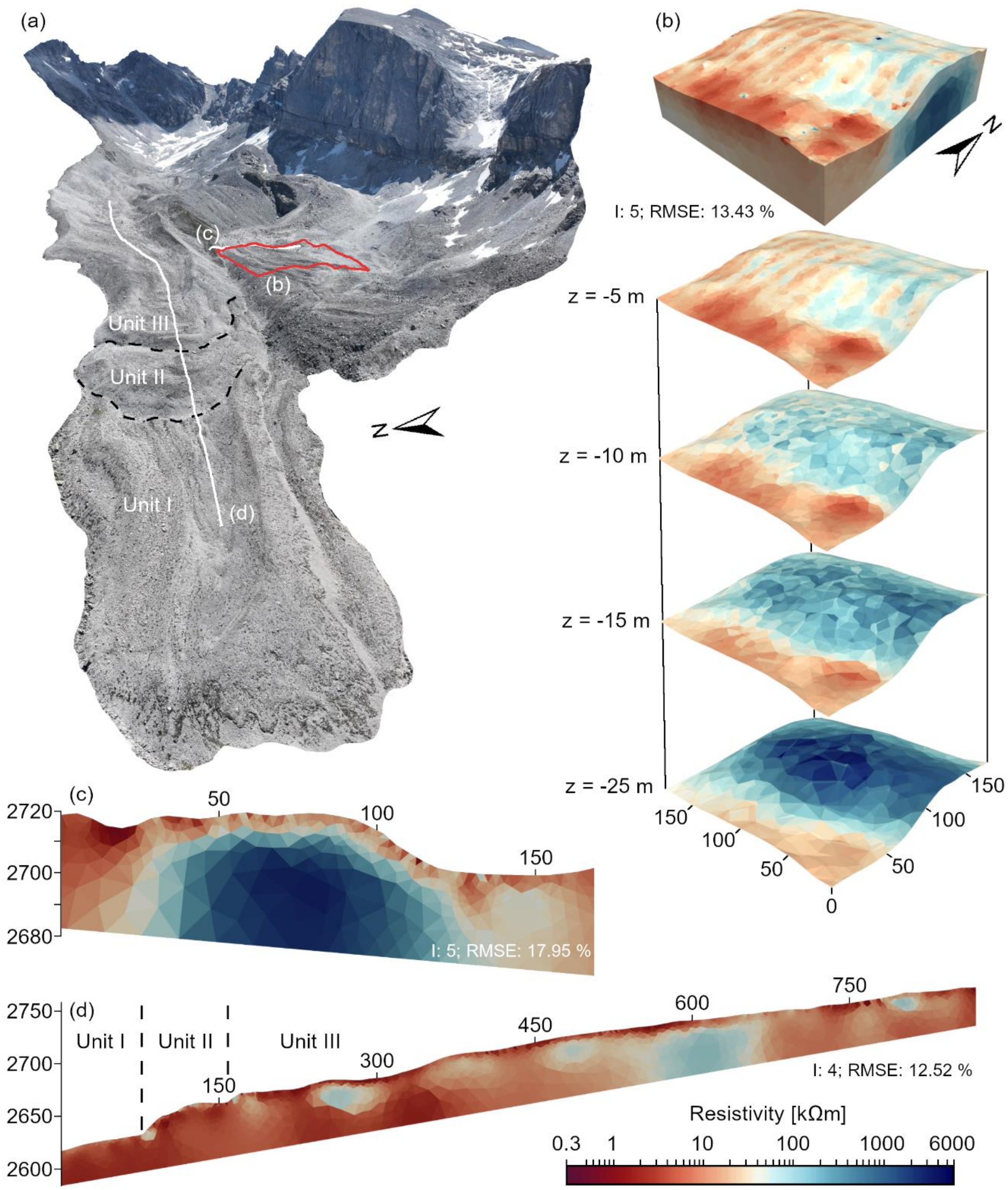


215 **Figure 2: ERT surveys in the Pipji glacier forefield. An overview of the survey location is given in (a). A quasi-three-dimensional ERT grid is shown in (b), whereas a two-dimensional cross profile of the thrust moraine complex and a longitudinal profile along the rock glacier are shown in (c) & (d).**

https://doi.org/10.5194/egusphere-2025-1671
Preprint. Discussion started: 15 May 2025


In comparison to the moraine complex, a two-dimensional ERT profile along the rock glacier to the north showed differing subsurface structures within its subunits (Fig. 2 d). The profile revealed a more heterogeneous resistivity distribution within the rock glacier. Larger high-resistive zones were detected between 240 m and 300 m, 350 m and 410 m, as well as between 460 m and 670 m of the profile. These structures start in depths between 5 m and 10 m below the surface and are about 20 m to 25 m thick. Only the larger one between 550 m and 670 m of the profile reaches greater depth and its lower boundary could not be detected. Resistivities in these structures are between 50 kΩm and 110 kΩm, and therefore more than one order of magnitude lower than in the area of the moraine complex. The resistivity range suggests the presence of permafrost within the subsurface of the rock glacier; however, the type and quantity of ground ice likely differ from those in the moraine. While resistivities above 1 MΩm are indicative of sedimentary or glacial ice, resistivities around 100 kΩm indicate ice-rich permafrost but the absence of buried glacier ice (cf. Haeberli and Vonder Mühll, 1996; Kneisel, 2006).

In the Oberferden Valley, a similar setup was chosen, meaning that a two-dimensional cross profile, as well as a quasi-three-dimensional grid were measured on the moraine complex and a longitudinal two-dimensional profile on the rock glacier. In the moraine complex, ERT measurements (Fig. 3) revealed a complex distribution of subsurface resistivities and a two- or three-layered internal structure. The upper part of the moraine complex shown in Fig. 3 (a, b) is underlain by an about 5 m thick, low-resistive surface-parallel layer (< 10 kΩm) and a high-resistive core (100 - 300 kΩm) below. The high resistivities indicate the presence of ice-rich permafrost. As visible in the three-dimensional model, this high-resistive zone starts at about 10 m depth and reaches down to the lower boundary of the model (30 m depth) and beyond. Especially in the 15 m depth layer, some structures are more resistive compared to the surrounding. They are aligned parallel to the dominant ridge at the surface. Further downslope, in the proximal flank of the moraine complex, resistivity values drop to a lower level and are in a range between 7 and 10 kΩm also at greater depth, indicating the absence of permafrost. However, a further but smaller high-resistive anomaly is notable in the lower area of the moraine flank (profile Fig. 3 b, 120 to 160 m), which is characterized by resistivity values between 50 and 100 kΩm and therefore also probably indicates frozen conditions. The overlying low-resistivity layer is slightly thicker in the lower part of the moraine flank and is around 6 m deep. The area between the two glacial lakes seems to be unfrozen, which is indicated by the low electrical resistivity values (< 5 kΩm) in all depth levels (see Fig. 3 b). The eastern part of the moraine complex is characterized by a more distinct surface morphology with a higher number of ridges. In this area, the ERT measurements revealed a zone of very high resistivities about one order of magnitude higher than in the upper, central and western parts of the complex (Fig. 3 c). Resistivities of more than 1 MΩm indicate the presence of sedimentary ice within the moraine complex. This detected structure fits well with observations made in the field in late summer 2022, where massive sedimentary ice could be observed in a thermo-erosional cave in the distal flank of the moraine (see also Fig. 3 & Fig. A1 b, d).

https://doi.org/10.5194/egusphere-2025-1671
Preprint. Discussion started: 15 May 2025


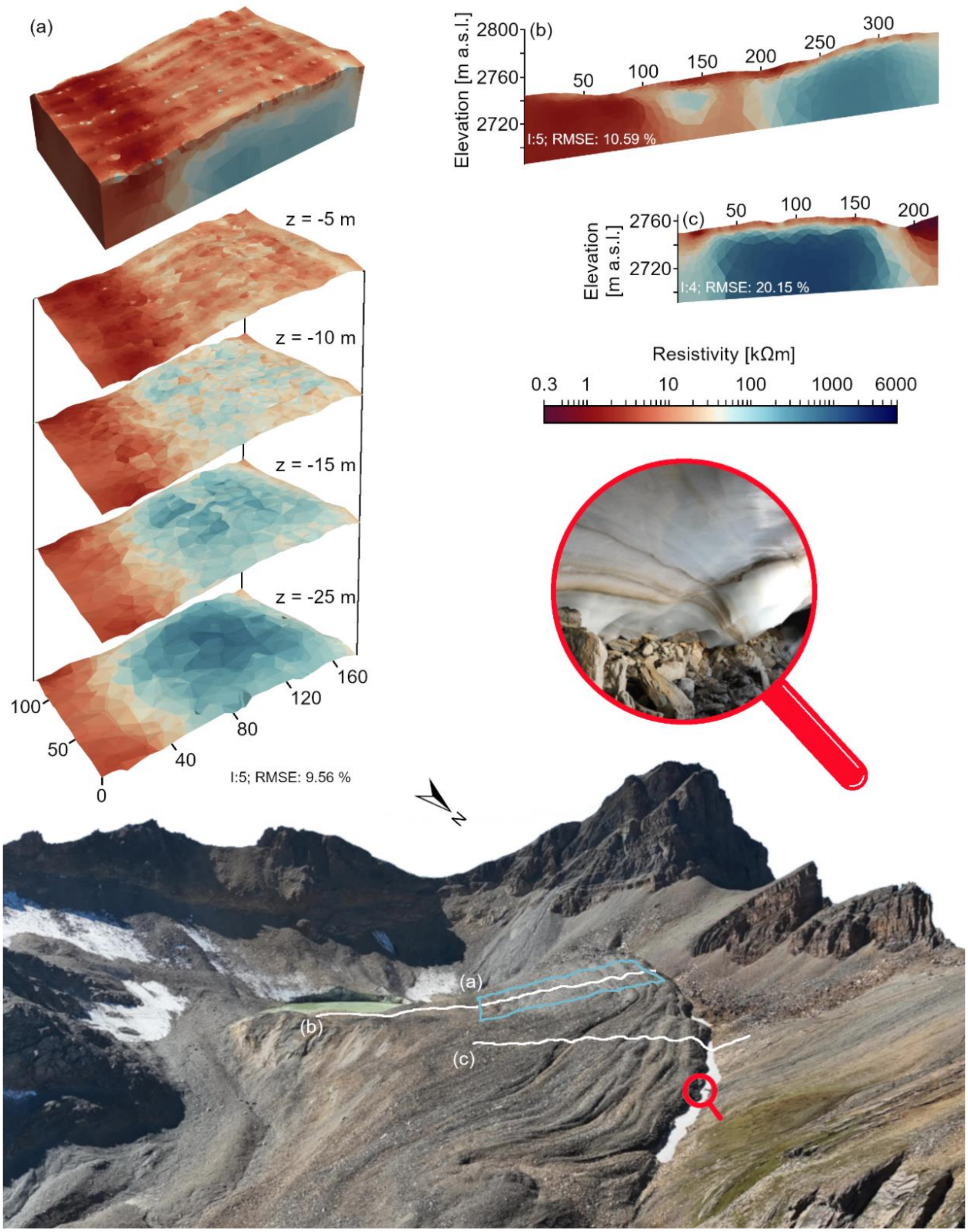


**Figure 3: ERT surveys on the Oberferden thrust moraine complex. A quasi-three-dimensional model is shown in (a), whereas two two-dimensional cross profiles are shown in (b) and (c). The locations of the ERT surveys are shown in the background image. The magnifier shows an outcrop of massive ice in a thermo-erosional cave in the distal moraine flank (see also Fig. A1 b, d).**

https://doi.org/10.5194/egusphere-2025-1671
Preprint. Discussion started: 15 May 2025


In comparison to this, two ERT profiles were conducted also on the neighbouring rock glacier further down the valley (see Fig. 4). The two cross profiles of the rock glacier showed comparable structures in the upper and lower parts of the rock glacier. In both profiles, a low-resistive upper layer (5 - 6 m thick) and high resistivity values (100 - 200 kΩm) below were detected within the orographic right (southern) half of the rock glacier. In contrast to this, the orographic left (northern) side is underlain by resistivities lower than 3.5 kΩm in the upper and 7 kΩm in the lower part of the rock glacier. These results indicate that today permafrost is only present in the right half of the rock glacier. The boundary between the two different subsurface structures fits well with the substrate boundary at the surface. The coarse-grained, talus-derived material seems to be underlain by permafrost, whereas the finer-grained moraine material in the left half seems to be free of permafrost.

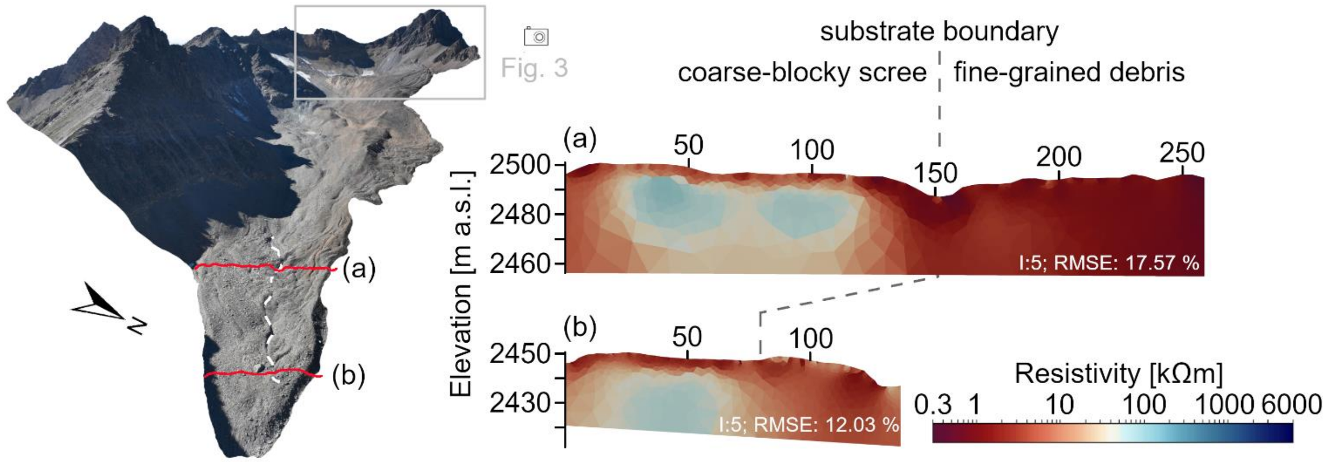


**Figure 4: ERT surveys on the Oberferden rock glacier. Position of the substrate boundary is highlighted by the dashed white line on the rock glacier surface. Image extent of Fig. 3 is also marked for orientation by the grey box.**

### 4.2 Surface dynamics and their relationships to the internal structure

Looking at the surface displacements derived from the DInSAR approach (Fig. 5), distinct displacement patterns are visible in both study areas. These are clearly linked to the geomorphological landform units of the individual rock glaciers and moraine complexes. Areas affected by layover or shadow in one of the orbits were masked out and are shown in grey. In Pipji Valley it is obvious that the rock glacier and the moraine complex are characterized by different displacement rates. The rock glacier in the north is mainly dominated by a westward displacement of up to 0.5 m/a (Fig. 5 a), whereas elevation changes are relatively low (Fig. 5 c). These vertical changes are patchier than the horizontal displacement pattern and do not exceed ±0.2 m/a except for an area of uplift in the central area of rock glacier unit III.

In contrast to this, the thrust moraine complex is characterized by only small horizontal displacement in the east-west direction (< 0.2 m/a), but by intense, negative elevation changes of up to -0.35 m/a. These are detectable nearly over the entire moraine complex and the spatial pattern is comparatively homogeneous. Looking at the seasonal variation of the surface displacement – derived from early and late season displacement rates – also distinct differences between the two landforms are visible. The

https://doi.org/10.5194/egusphere-2025-1671
Preprint. Discussion started: 15 May 2025


moraine complex is characterized by a high seasonality (bright blue to turquoise colours), which means that there is only low or even no movement in the early snow-free summer season and a medium to high movement during the late snow-free summer season. This characteristic is an areawide phenomenon of the moraine complex with only some isolated spots of lower seasonality, characterized by generally low displacement rates. Conversely, the rock glacier only shows a high seasonality in its orographic right part, which is also part of the former lateral moraine. Besides, the rock glacier shows lower seasonality, which is indicated by the dark blue and magenta colours. Thus, rock glacier movement exhibits notably less seasonal variation compared to the movement of the neighbouring moraine complex.

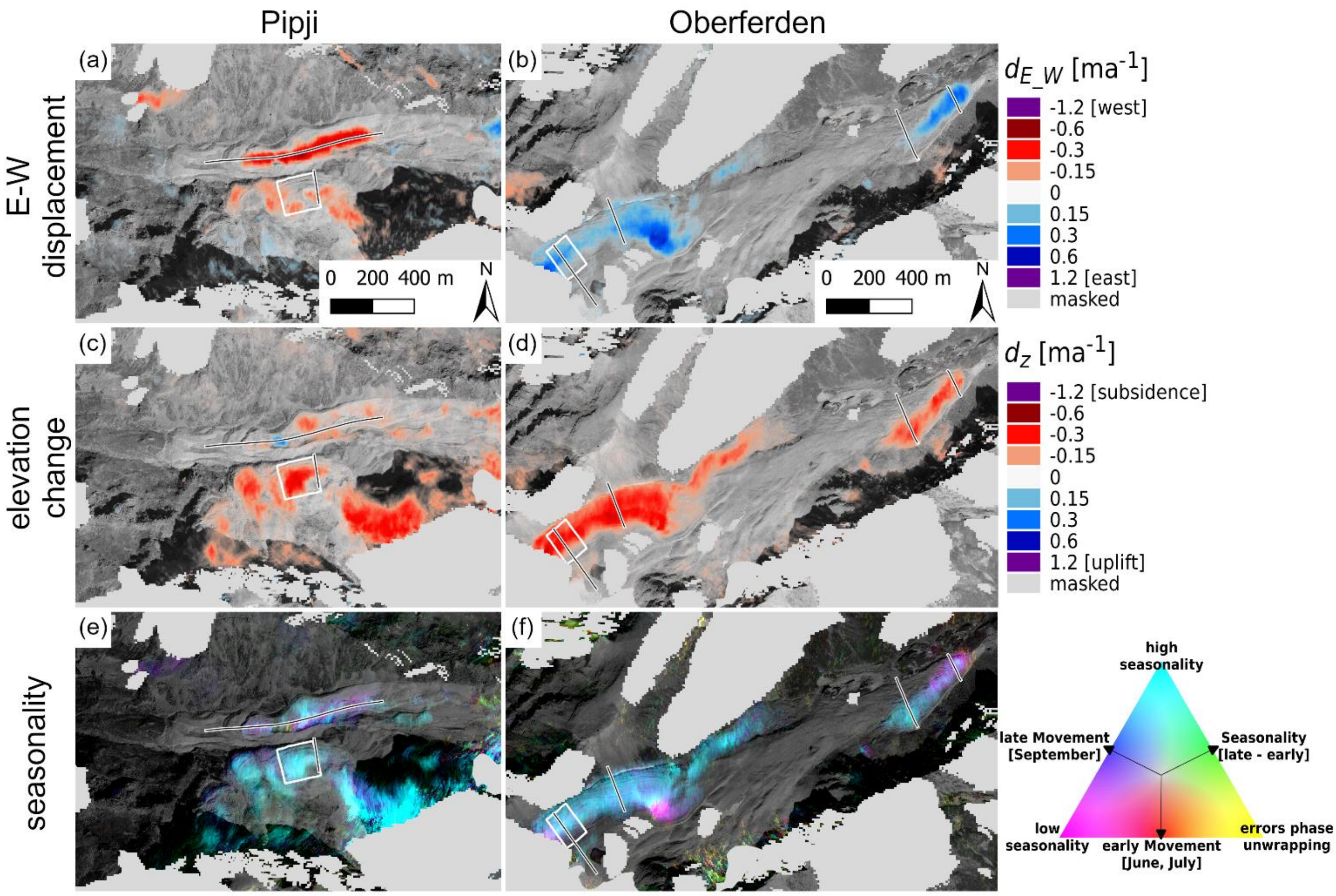


**Figure 5: InSAR-based analysis of surface morphodynamics in the Pipji (left column) and Oberferden (right column) glacier forefields for the period 2017 - 2021. The upper panels show the surface displacement in the east-west direction, the central panels the vertical displacement, and the lower panels the seasonality derived from early and late season movements. The locations of all ERT surveys are also shown in the maps.**

Similar spatial patterns in displacement rates are evident in the Oberferden glacier forefield. Similarly, the moraine complex in this area is characterized by negative elevation changes ranging from -0.2 to -0.5 m/a, affecting nearly the entire complex.

https://doi.org/10.5194/egusphere-2025-1671
Preprint. Discussion started: 15 May 2025


The spatial pattern of horizontal displacements shows some differences with higher horizontal displacement rates (up to 0.5 m/a) in the steeper eastern section of the complex but only lower horizontal displacements (< 0.3 m/a) in flatter areas. Also, regarding the seasonality (Fig. 5 f) the Oberferden moraine complex shows similar characteristics as the Pipji moraine complex and is characterized by comparatively high seasonality, so low early snow-free season and intense late snow-free season movement. An exception is the very steep section in the east (magenta-colored area), where higher displacements are observed early in the summer season, leading to reduced seasonal variation. Further down the valley, the rock glacier exhibits spatially heterogeneous displacement patterns, with detectable movement occurring only in the orographic right half of the glacier. In this area, both horizontal as well as negative elevation change are detectable in a similar range (0.1 - 0.35 m/a) with increasing horizontal displacement towards the front. In the upper part, close to the source area of the rock glacier, only elevation changes occurred during the investigated period. The rock glacier is also characterized by different seasonal patterns. While the upper part with only vertical displacement shows rather high seasonality, the lower part with horizontal displacement shows a more balanced behaviour and less seasonality throughout the summer.

Comparing the detected spatial movement patterns and seasonal dynamics with subsurface information from ERT highlights notable correlations. When analyzing individual profiles, a strong correlation is evident between surface displacement (in both directions) and the maximum resistivity beneath each pixel. Along the long cross-profile of the Oberferden moraine complex (Fig. 6 b, d), the correlation between the logarithm of maximum resistivity and absolute displacement in the east-west direction reaches a coefficient of determination ($R^2$) of 0.75* (Fig. 6 j), while its correlation with elevation change results in an $R^2$ of 0.76* (Fig. 6 f). Similar trends are observed in the Pipji moraine complex when considering individual profiles. However, along the longitudinal profile of the Pipji rock glacier, correlations between these parameters are notably weak ($R^2 < 0.25$) and, moreover, not all significant (cf. Fig. 6 a, c, e, g, h).

To obtain more generalized insights, this analysis was conducted for all data points across all two-dimensional profiles. In Fig. 7 (a, c, e), maximum resistivity values are plotted against three morphometric parameters, categorized by landform type. For all three parameters, correlations are notably stronger within moraine complexes (red) compared to rock glaciers (grey). This suggests that the morphodynamics of moraines are more consistently influenced by internal structures and, consequently, by ice content, whereas rock glaciers exhibit greater variability. In Fig. 7 (b, d, f), the distributions of vertical elevation change (b), horizontal displacement (d) and seasonality (e) are shown for all four classes as violin plots. This enables a direct comparison of the morphodynamics for the respective subunits of the individual landforms and should reveal some linkages with permafrost properties for both kinds of landforms. Looking at a general comparison of rock glaciers (grey) and moraine complexes (red), it is striking that the morphodynamic parameters for sample points on the moraine features are characterized by a lower scattering within each class. Especially in the two low- or lower-resistive groups representing no or ice-poor permafrost, moraines are less affected by morphodynamics than the rock glaciers. Only some points on the rock glaciers appear to be subject to considerable movement, although they are underlain by no or very ice-poor permafrost. Striking is the bimodal distribution of horizontal displacement in the second class for the rock glacier data points, indicating two different dominating displacement regimes within this class. On the moraine complexes in general, the relationship follows an expected pattern in

https://doi.org/10.5194/egusphere-2025-1671
Preprint. Discussion started: 15 May 2025


which higher resistivities (probably also higher ice contents) mean higher morphodynamics and seasonal variation. This is valid, especially for the vertical movement and the seasonality, but also concerning the horizontal displacement in parts.

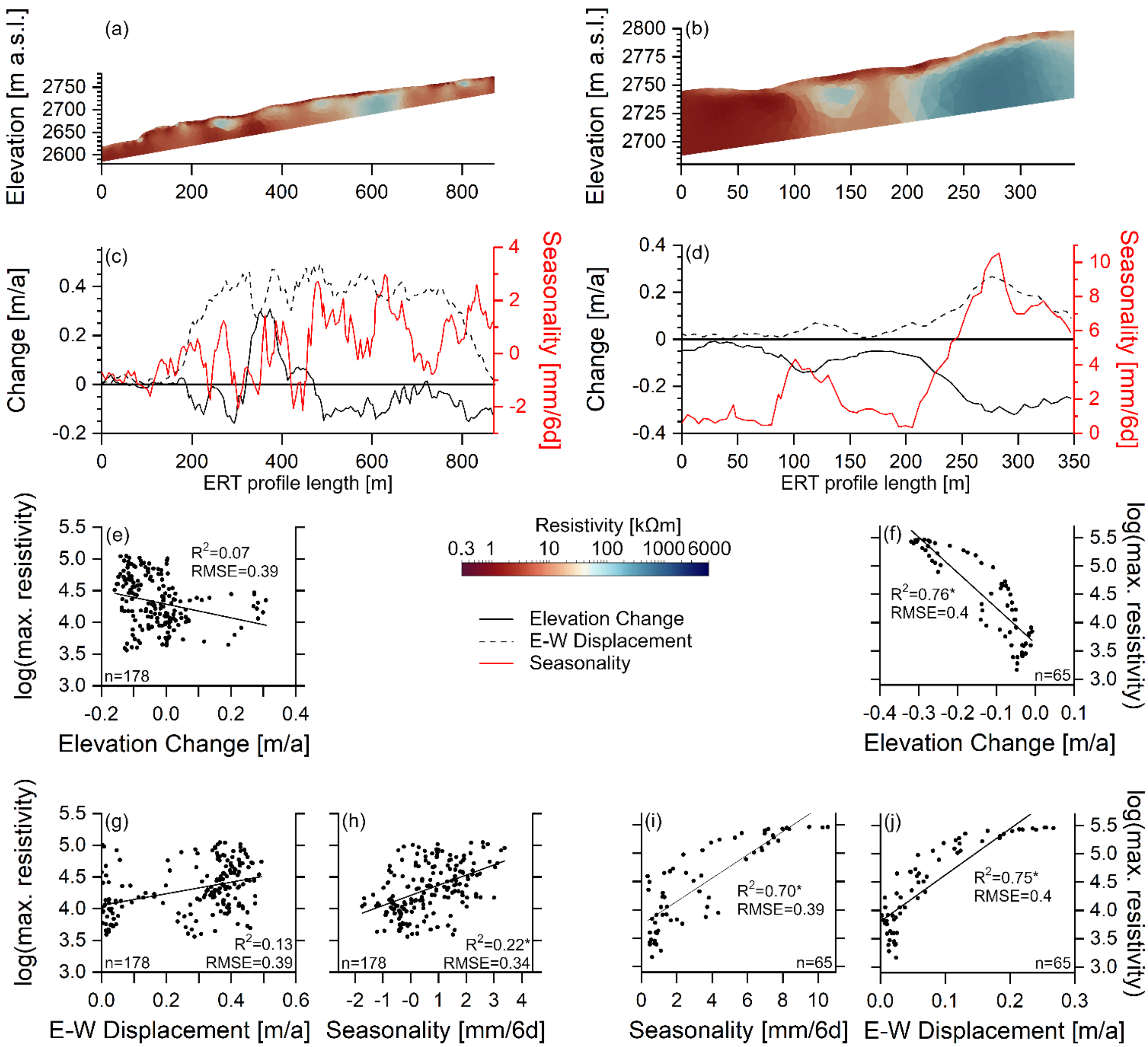


**Figure 6: Comparison of the ERT pseudo sections ((a) & (b)) with DInSAR-derived elevation change, horizontal displacement and seasonality ((c) & (d)) along the longitudinal profile of the Pipji rock glacier ((a) & (c)) and the cross profile of the Oberferden moraine complex ((b) & (d)). In the subplots (e) to (j), the individual scatterplots for the relationships are shown. "*" indicates the significance of the respective correlation (α = 5%).**

https://doi.org/10.5194/egusphere-2025-1671
Preprint. Discussion started: 15 May 2025


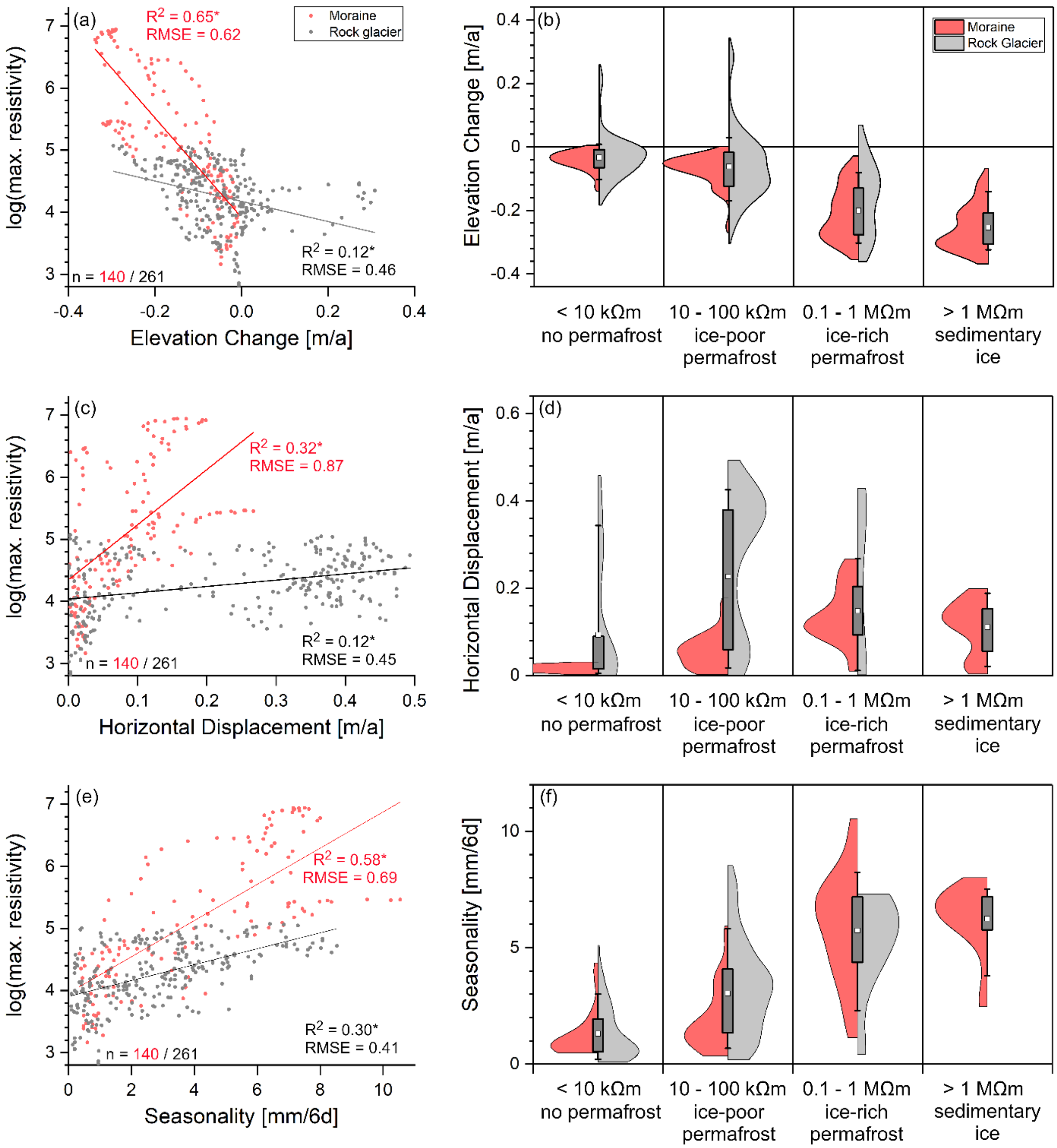


340 **Figure 7: Comparison of InSAR-detected elevation change, horizontal displacement and seasonality with the logarithm of maximum resistivity (in Ωm) below each respective pixel along all two-dimensional ERT profiles. In the left column, the logarithm of the maximum resistivity is plotted against the elevation change (a), horizontal displacement (c) and seasonality (e), while in the right column, the distribution of each parameter is shown for four different resistivity classes (b, d, e). "*" indicates the significance of the respective correlation (α = 5%).**

## 5 Discussion

### 5.1 Methodological approach

ERT has been widely used in this field of research for more than 20 years; however, its application to coarse-blocky landforms and ice-rich environments remains challenging and requires further discussion. Coarse-grained materials as common on rock glaciers and alpine thrust moraine complexes affect the ground coupling of the electrodes due to the lack of fine-grained, conductive sediments. Therefore, ground coupling was enhanced using water-soaked sponges as recommended for such environments (Herring et al., 2023; Vonder Mühll, 1993). Nevertheless, all measured quadrupoles had to be checked regarding their stack deviation and bad datum points (deviation > 5%) were deleted prior to inversion. Raw data quality was generally acceptable, but in total about 10 % of the data points had to be deleted. In the Oberferden glacier forefield, data quality remained relatively consistent across profiles, with approximately 8% of datum points removed. In contrast, data quality in the Pipji glacier forefield was more variable, with a maximum of 23% and an average of 12% of datum points removed per profile. In addition to the limitation due to the ground coupling, there are also the very heterogeneous subsurface properties and the extreme range of resistivity values due to the different materials (< 300 Ωm to > 6 MΩm), which make modelling difficult and lead to comparatively high RMS errors. Also, the absolute resistivity values within high-resistive structures (> 1 MΩm) should be interpreted with caution due to the lower sensitivity resulting from low currents within the high-resistive zones (e.g. Hilbich et al., 2009; Marescot et al., 2003). The setup of the quasi-three-dimensional grids was adapted to the research question and the local conditions. Fourfold electrode spacing was used as interline spacing, which is higher than recommended by Gharibi and Bentley (2005) or Rödder and Kneisel (2012b), for example, but seems to be enough to detect the differences in the large-scale structure of the moraine complexes. Profiles were only measured in parallel, as perpendicular profiles could be omitted due to the good consistency of the profiles and the expected subsurface structures.

Concerning the DInSAR approach used, there is already a detailed discussion of the method by Buchelt et al. (2023) and Buchelt et al. (2024). Nevertheless, some aspects need to be mentioned in terms of the application of the DInSAR approach, particularly from a geomorphological perspective. One limitation is the inability to detect the north-south horizontal displacement component due to sensor orientation, meaning surface movements in this direction cannot be confirmed or excluded. At both study sites, the predominant orientation of the landforms follows an east-west direction. However, in the moraine complex areas, north-south movement is also expected due to the known back-creep of such landforms toward the glacier forefield (cf. Kneisel and Kääb, 2007; Wee and Delaloye, 2022). Further, velocities from DInSAR are restricted to snow-free summer months, covering only about one-third of the year. To estimate annual rates, the stacked results were multiplied by factor three. However, previous studies (e.g., Wirz et al., 2016; Cicoira et al., 2022) have shown slower winter velocities, suggesting that this extrapolation likely overestimates annual movement, particularly in areas with high seasonal variability – often regions dominated by subsidence. This is also relevant to DInSAR-derived seasonality, which captures only the variability within the snow-free months, missing early acceleration during snowmelt when water infiltrates shear horizons (Kenner et al., 2017, 2020; Wirz et al., 2016).

Another factor to consider is the masking of areas lacking reliable data due to layover and shadow effects. However, these limitations are minimal within the investigated landforms. This issue is particularly negligible when comparing with geophysically detected subsurface structures, as neither the moraine complexes nor the rock glaciers are affected. Phase unwrapping errors, which typically limit the accuracy of velocity measurements in fast-moving areas, were not detected in the investigated regions, except for a very small area on the Pipji rock glacier, where they cannot be ruled out.

The integration of remote sensing and geophysical measurements to analyze interactions between surface and subsurface processes has been rarely applied in Alpine permafrost research. However, as the results demonstrate, this combination offers valuable advantages, enabling the high-resolution spatial measurement of surface parameters while simultaneously providing multi-dimensional subsurface information. This can contribute to a better understanding of the morphodynamics of landforms and the associated processes, both recent and in the future. This way, the respective methodological advantages can be combined, although the methodological weaknesses must not be neglected for each approach. Therefore, we should note that this combined approach of geophysical and DInSAR data is still relatively new and little comparable data is available so far.

### 5.2 Glacier-permafrost interactions and related recent morphodynamics

The coexistence of glaciers and permafrost distinctly shaped the geomorphology of both glacier forefields and their adjacent areas. Especially the thrust moraine complexes investigated in the current study indicate not only a coexistence but also an interaction between glaciers and permafrost. The geoelectrical surveys conducted on both complexes revealed similar internal structures and enabled a delineation of different morphological subunits, confirming the glacier-permafrost interaction. Especially the incorporated blocks of massive ice of sedimentary origin within both moraines, revealed by very high electrical resistivity values > 1 MΩm, are a distinct hint of that (Haeberli and Vonder Mühll, 1996; Kneisel et al., 2000; Kneisel, 2003). In addition, high-resistive zones (0.1 – 1 MΩm) indicate the presence of ice-rich permafrost but potentially the absence of massive, sedimentary ice or a polygenetic type of ground ice in the upper part of the Oberferden moraine complex. Additional GPR measurements conducted in this area (not shown) also reveal the presence of shear planes resulting from glacial thrusting within these high-resistive and ice-rich permafrost zones. Similar internal structures were already reported from other thrust moraine complexes by Kunz et al. (2022) and Kunz and Kneisel (2020). The recent morphodynamics on the investigated landforms seem to be dominated by negative vertical changes indicating a thinning due to deformation but also degradation of ice-rich permafrost and melt-out of massive ice as also described by Wee and Delaloye (2022) and Wee et al. (2024). This is also supported by the strong seasonality, which states larger displacements only during the warm summer months and not during the early summer season when energy from heat fluxes is used for melting snow and seasonal ice in the active layer (Amschwand et al., 2024a; Scherler et al., 2014). Horizontal movement is less intense and restricted to the steeper parts, although the missing north-south component should not be ignored. Especially the morphological orientation of the two moraine complexes and the former ice flow direction and therefore the direction of glacial thrusting suggests that at least the backward creep described in the few available studies (cf. Kneisel and Kääb, 2007; Kunz et al., 2022; Wee and Delaloye, 2022) could also have a north-south component.

The two investigated rock glaciers dominate the lower elevated parts of the late-glacial and LIA glacier forefields and at least partly originate from moraine deposits of the respective glaciers. In the Pipji Valley, the rock glacier evolved entirely from the former glacier and its moraine deposits (Tatenhove and Dikau, 1990), but the surface morphology indicates different development stages and phases of activities, as also reported by Otto et al. (2009). The Oberferden rock glacier is only partly moraine-derived, and the different origins of the host materials seem to have a major impact on the recent state of the rock glacier. Within the moraine-derived orographic left half, low resistivity values indicate the absence of permafrost and the DInSAR approach could not detect any movement either. In contrast, the orographic right side of the rock glacier, which was formed from coarse blocky scree, shows high electrical resistivity and also distinct movement that indicate the presence of ground ice in the subsurface. The main reason for this internal disbalance might be the substrate characteristics and the related favourable thermal conditions within the coarse-blocky material (Amschwand et al., 2024b; Harris and Pedersen, 1998; Rödder and Kneisel, 2012a), but also shading could strengthen the effect at this site (microclimate). The different behaviour in the upper and lower part of this rock glacier might indicate the typically steadier permafrost creep within the lower part of the lobe and rather mass loss during the warm summer months in the upper part. The area of uplift on the Pipji rock glacier (cf. Fig 5 c) indicates compressive flow (cf. Haeberli et al., 2006) due to higher rock glacier velocities in the upper part and lower velocities in the lower units (Unit I & II). However, values are probably partially altered by phase unwrapping artefacts in descending orbit as this is the fastest moving part of the rock glacier. The different velocities, in turn, are likely due to the different ice contents indicated by the ERT measurements.

When comparing the thrust moraines and the neighbouring rock glaciers, the differences regarding their internal structure are prominent. Both rock glaciers show more heterogeneous structures with higher variabilities of the electrical resistivities and smaller, more isolated high-resistive zones. In contrast, the thrust moraines are both underlain by large, very high-resistive, more coherent zones indicating a more homogeneous internal structure. Besides, the DInSAR-derived surface displacement shows some distinct differences in the morphodynamics of the two landform types: Negative elevation change dominates in the area of the moraines, whereas the horizontal displacement component predominates in the area of the rock glaciers. Also, the moraine complexes are characterized by distinctly higher seasonality than the neighbouring rock glaciers, meaning that surface displacement varies stronger throughout the snow-free summer months. These findings fit well with recent observations by Haeberli et al. (2024) and Wee et al. (2024) that report different morphodynamics of landforms depending on ice content and involved ice type. The differences between the two landform types, which are highlighted by the statistical differences presented in Fig. 7, might be mainly caused by the different processes of movement. Within rock glaciers, internal deformation and shearing result in permafrost creep (Arenson et al., 2002; Cicoira et al., 2021; Gärtner-Roer et al., 2022). These processes can also take place in less ice-rich areas or at least be transferred to them and are mainly driven by permafrost temperatures near the shear horizon (hence, rather low seasonality). This results in lower correlations between movement parameters and subsurface resistivity. In the area of the thrust moraines – at least in the areas that are no longer subject to back creep – the movement is mainly due to the melting of the ice (cf. Wee et al., 2024; Wee and Delaloye, 2022), which is characterized by less horizontal displacement, primarily negative elevation changes that increase with higher ice contents and higher seasonality due to the strongest thaw subsidence during the late summer. This would explain why the morphodynamics of the moraines correlate stronger with the electrical resistivity than in the area of the rock glaciers. The effect of thaw subsidence is highest in ice-rich environments, which in turn are characterized by the highest electrical resistivity values. Within the rock glacier, permafrost creep is affected but not totally dependent on the ice content, which is why the relationship between surface morphodynamics and subsurface resistivity is considerably weaker. However, it should be noted that the processes can of course also take place in the other respective landform, but they are not dominant there.

These findings highlight the importance of correct distinction between these two landform types, even if this is sometimes very complex to accomplish. It is true that morphologically they have a kind of similar appearance, their occurrence is often limited to the same environments and both landform types are characterized by strong morphodynamics. Nevertheless, the internal structures and the morphodynamical characteristics can be different based on our presented data. Hence, our findings could be used to better differentiate between these adjacent landforms:

DInSAR-derived movement patterns can be used to identify ice-rich glacial or periglacial landforms at a larger spatial scale, whereas geophysical surveys could help to clarify internal structures. This is of special importance, as so far no distinction has been made between thrust moraines and rock glaciers in many rock glacier inventories (Bertone et al., 2022; Nyenhuis, 2005; Rock glacier inventories and kinematics (RGIK), 2023). However, such a differentiation would be of high importance as the primary underlying process for the morphodynamics is different (melting of ice vs. permafrost creep). As morphodynamical parameters such as rock glacier velocity are derived as essential climate variable (ECV) based on such inventories (Hu et al., 2025; Streletskiy et al., 2021; World Meteorological Organization (WMO), 2022), a lack of distinction between the different landforms may lead to a distortion of the parameters and thus of the assessment of morphodynamic changes in the context of climate change.

## 6 Conclusions

The combined approach of geophysical surveying and remote-sensing-based surface displacement analysis enabled the investigation of relationships and linkages between the subsurface structures of thrust moraine complexes and rock glaciers with their recent morphodynamics. The use of two- and quasi-three-dimensional electrical resistivity tomography (ERT) revealed the recent distribution of ground ice and permafrost occurrences, respectively, but also enabled the differentiation of different kinds of ground ice and permafrost within the two investigated glacier forefields. The use of Differential Interferometry Synthetic Aperture Radar (DInSAR) enabled a high-resolution derivation of surface displacements on both landform types, thrust moraines and rock glaciers. The main findings of the combined approach are as follows: (i) Glacier-permafrost interactions resulted in the incorporation of large blocks of massive ice of sedimentary origin into the thrust moraine complexes. Resistivity distribution and, therefore, probably the ground ice distribution within the rock glaciers is much more heterogeneous and characterized by rather small-scale structures. Different resistivity ranges indicate the presence of different ground ice types within the two investigated landform types. (ii) Both landforms are characterized by distinct recent surface

https://doi.org/10.5194/egusphere-2025-1671
Preprint. Discussion started: 15 May 2025


morphodynamics in both study areas. On the moraine complexes, these are dominated by negative vertical changes and high seasonality. On the adjacent investigated rock glaciers, they are more balanced between vertical and horizontal changes and lower seasonality was detected. (iii) A strong correlation between subsurface resistivity – representing subsurface structure such as ice content and type – and recent morphodynamics in the area of the moraine complexes highlights intense relationship between these characteristics. The dominance of negative elevation changes and high seasonality indicate that displacements result mainly from melt of massive ice within the thrust moraine complexes. The significantly lower correlation between the parameters in the area of the rock glaciers has to be interpreted as signal from the internal rock glacier dynamics, which are not entirely controlled by the ice content and also not fully understood yet.

Conclusively, distinguishing between thrust moraines and rock glaciers is essential due to their distinct internal structures and morphodynamic processes, despite their sometimes-similar appearance and shared environmental settings in alpine environments. DInSAR-derived movement patterns support large-scale identification, while geophysical surveys provide critical clarification regarding the internal structure and origin of glacial and periglacial landforms. Since many rock glacier inventories do not yet differentiate between these landforms, this omission may lead to inaccuracies in assessing morphodynamic changes, particularly when rock glacier velocity is used as an essential climate variable.

These findings from our combined methodological approach could enhance our understanding of past, present, and future landscape evolution in high-alpine environments. The clear differences between rock glaciers and thrust moraines emphasize the need for morphological distinction, particularly when evaluating movement rates in climate-related studies. Methodologically, this study underscores the advantages of integrating geophysical and remote-sensing-based approaches to analyze complex interactions between surface and subsurface characteristics. This combined approach is especially valuable in the context of climate change, enabling a more precise assessment of evolving periglacial landscapes.

https://doi.org/10.5194/egusphere-2025-1671
Preprint. Discussion started: 15 May 2025


**Appendix**


**Figure A1: Sedimentary ice outcrops in the investigated thrust moraine complexes. In (a) and (c), an ice outcrop in the proximal flank of the Pipji thrust moraine complex is shown. In (c), internal shear planes with incorporated sediments are visible. Images were taken in July 2024 by Antje Verheyen. (b) and (d) present an ice outcrop in the distal flank of the Oberferden thrust moraine complex. In (d), the sedimentary structures of the ice are visible. Images were taken in September and October 2022 by Christof Kneisel and Julius Kunz.**

## Data availability

All data are available upon request.

**Author contributions**

CK and JK designed the research concept, while CK, TW, SB, and JK conducted the associated field measurements. SB, TW, and JK carried out data processing and analysis. JK prepared the manuscript with contributions from all co-authors. CK and TU provided funding and logistics.

**Competing interests**

The authors declare that they have no conflict of interest.

**Acknowledgements**

Acquiring the geophysical data sets in such an environment is quite labour-intensive and exhausting. Therefore, we thank our field assistants Jannik Schönfeld, Antje Verheyen, Judith Hartwich, Severin Scheib as well as the participants of the field courses 04-Geo-MPG 2 (2023 & 2024) and the EAGLE master's field course 2023 for their tireless efforts; this study would not have been possible without their help. Thanks to the EU and the Copernicus Program for making Sentinel-1 data freely available.

**Financial support**

This project was funded by the Deutsche Forschungsgemeinschaft (DFG, German Research Foundation) – 506183115.

**References**

Amschwand, D., Tschan, S., Scherler, M., Hoelzle, M., Krummenacher, B., Haberkorn, A., Kienholz, C., Aschwanden, L., and Gubler, H.: On the hydrological significance of rock glaciers: A case study from Murtèl rock glacier (Engadine, eastern Swiss Alps) using below-ground energy-flux measurements, ground-ice melt observations and hydrological measurements, https://doi.org/10.5194/egusphere-2024-844, 18 April 2024a.

Amschwand, D., Scherler, M., Hoelzle, M., Krummenacher, B., Haberkorn, A., Kienholz, C., and Gubler, H.: Surface heat fluxes at coarse blocky Murtèl rock glacier (Engadine, eastern Swiss Alps), The Cryosphere, 18, 2103–2139, https://doi.org/10.5194/tc-18-2103-2024, 2024b.

Arenson, L., Hoelzle, M., and Springman, S.: Borehole deformation measurements and internal structure of some rock glaciers in Switzerland, Permafrost & Periglacial, 13, 117–135, https://doi.org/10.1002/ppp.414, 2002.

Bertone, A., Barboux, C., Bodin, X., Bolch, T., Brardinoni, F., Caduff, R., Christiansen, H. H., Darrow, M. M., Delaloye, R., Etzelmüller, B., Humlum, O., Lambiel, C., Lilleøren, K. S., Mair, V., Pellegrinon, G., Rouyet, L., Ruiz, L., and Strozzi, T.: Incorporating InSAR kinematics into rock glacier inventories: insights from 11 regions worldwide, The Cryosphere, 16, 2769–2792, https://doi.org/10.5194/tc-16-2769-2022, 2022.

Biskaborn, B. K., Smith, S. L., Noetzli, J., Matthes, H., Vieira, G., Streletskiy, D. A., Schoeneich, P., Romanovsky, V. E., Lewkowicz, A. G., Abramov, A., Allard, M., Boike, J., Cable, W. L., Christiansen, H. H., Delaloye, R., Diekmann, B., Drozdov, D., Etzelmüller, B., Grosse, G., Guglielmin, M., Ingeman-Nielsen, T., Isaksen, K., Ishikawa, M., Johansson, M., Johannsson, H., Joo, A., Kaverin, D., Kholodov, A., Konstantinov, P., Kröger, T., Lambiel, C., Lanckman, J.-P., Luo, D., Malkova, G., Meiklejohn, I., Moskalenko, N., Oliva, M., Phillips, M., Ramos, M., Sannel, A. B. K., Sergeev, D., Seybold, C., Skryabin, P., Vasiliev, A., Wu, Q., Yoshikawa, K., Zheleznyak, M., and Lantuit, H.: Permafrost is warming at a global scale, Nat Commun, 10, 264, https://doi.org/10.1038/s41467-018-08240-4, 2019.

Blöthe, J. H., Halla, C., Schwalbe, E., Bottegal, E., Trombotto Liaudat, D., and Schrott, L.: Surface velocity fields of active rock glaciers and ice-debris complexes in the Central Andes of Argentina, Earth Surf Processes Landf, 46, 504–522, https://doi.org/10.1002/esp.5042, 2021.

Bosson, J., Deline, P., Bodin, X., Schoeneich, P., Baron, L., Gardent, M., and Lambiel, C.: The influence of ground ice distribution on geomorphic dynamics since the Little Ice Age in proglacial areas of two cirque glacier systems, Earth Surf Processes Landf, 40, 666–680, https://doi.org/10.1002/esp.3666, 2014.

Buchelt, S., Blöthe, J. H., Kuenzer, C., Schmitt, A., Ullmann, T., Philipp, M., and Kneisel, C.: Deciphering Small-Scale Seasonal Surface Dynamics of Rock Glaciers in the Central European Alps Using DInSAR Time Series, Remote Sensing, 15, 2982, https://doi.org/10.3390/rs15122982, 2023.

Buchelt, S., Kunz, J., Wiegand, T., and Kneisel, C.: Dynamics and internal structure of a rock glacier: Inferring relationships from the combined use of differential synthetic aperture radar interferometry, electrical resistivity tomography and ground-penetrating radar, Earth Surf Processes Landf, 49, 4743–4758, https://doi.org/10.1002/esp.5993, 2024.

Buckel, J., Mudler, J., Gardeweg, R., Hauck, C., Hilbich, C., Frauenfelder, R., Kneisel, C., Buchelt, S., Blöthe, J. H., Hördt, A., and Bücker, M.: Identifying mountain permafrost degradation by repeating historical electrical resistivity tomography (ERT) measurements, The Cryosphere, 17, 2919–2940, https://doi.org/10.5194/tc-17-2919-2023, 2023.

Chen, C. W. and Zebker, H. A.: Phase unwrapping for large SAR interferograms: statistical segmentation and generalized network models, IEEE Trans. Geosci. Remote Sensing, 40, 1709–1719, https://doi.org/10.1109/TGRS.2002.802453, 2002.

Cicoira, A., Marcer, M., Gärtner-Roer, I., Bodin, X., Arenson, L. U., and Vieli, A.: A general theory of rock glacier creep based on in-situ and remote sensing observations, Permafrost & Periglacial, 32, 139–153, https://doi.org/10.1002/ppp.2090, 2021.

Cicoira, A., Weber, S., Biri, A., Buchli, B., Delaloye, R., Da Forno, R., Gärtner-Roer, I., Gruber, S., Gsell, T., Hasler, A., Lim, R., Limpach, P., Mayoraz, R., Meyer, M., Noetzli, J., Phillips, M., Pointner, E., Raetzo, H., Scapozza, C., Strozzi, T., Thiele, L., Vieli, A., Vonder Mühll, D., Wirz, V., and Beutel, J.: In situ observations of the Swiss periglacial environment using GNSS instruments, Earth Syst. Sci. Data, 14, 5061–5091, https://doi.org/10.5194/essd-14-5061-2022, 2022.

Crippa, C., Franzosi, F., Zonca, M., Manconi, A., Crosta, G. B., Dei Cas, L., and Agliardi, F.: Unraveling Spatial and Temporal Heterogeneities of Very Slow Rock-Slope Deformations with Targeted DInSAR Analyses, Remote Sensing, 12, 1329, https://doi.org/10.3390/rs12081329, 2020.

Cusicanqui, D., Bodin, X., Duvillard, P., Schoeneich, P., Revil, A., Assier, A., Berthet, J., Peyron, M., Roudnitska, S., and Rabatel, A.: Glacier, permafrost and thermokarst interactions in Alpine terrain: Insights from seven decades of reconstructed dynamics of the Chauvet glacial and periglacial system (Southern French Alps), Earth Surf Processes Landf, 48, 2595–2612, https://doi.org/10.1002/esp.5650, 2023.

Eriksen, H. Ø., Rouyet, L., Lauknes, T. R., Berthling, I., Isaksen, K., Hindberg, H., Larsen, Y., and Corner, G. D.: Recent Acceleration of a Rock Glacier Complex, Ádjet, Norway, Documented by 62 Years of Remote Sensing Observations, Geophysical Research Letters, 45, 8314–8323, https://doi.org/10.1029/2018GL077605, 2018.

Etzelmüller, B. and Hagen, J. O.: Glacier-permafrost interaction in Arctic and alpine mountain environments with examples from southern Norway and Svalbard, Geological Society, London, Special Publications, 242, 11–27, https://doi.org/10.1144/GSL.SP.2005.242.01.02, 2005.

Fleischer, F., Haas, F., Piermattei, L., Pfeiffer, M., Heckmann, T., Altmann, M., Rom, J., Stark, M., Wimmer, M. H., Pfeifer, N., and Becht, M.: Multi-decadal (1953–2017) rock glacier kinematics analysed by high-resolution topographic data in the upper Kaunertal, Austria, The Cryosphere, 15, 5345–5369, https://doi.org/10.5194/tc-15-5345-2021, 2021.

Gärtner-Roer, I., Brunner, N., Delaloye, R., Haeberli, W., Kääb, A., and Thee, P.: Glacier–permafrost relations in a high-mountain environment: 5 decades of kinematic monitoring at the Gruben site, Swiss Alps, The Cryosphere, 16, 2083–2101, https://doi.org/10.5194/tc-16-2083-2022, 2022.

Gharibi, M. and Bentley, L. R.: Resolution of 3-D Electrical Resistivity Images from Inversions of 2-D Orthogonal Lines, JEEG, 10, 339–349, https://doi.org/10.2113/JEEG10.4.339, 2005.

Günther, T., Rücker, C., and Spitzer, K.: Three-dimensional modelling and inversion of dc resistivity data incorporating topography - II. Inversion, Geophysical Journal International, 166, 506–517, https://doi.org/10.1111/j.1365-246X.2006.03011.x, 2006.

Haeberli, W.: Holocene Push-Moraines in Alpine Permafrost, Geografiska Annaler. Series A, Physical Geography, 61, 43, https://doi.org/10.2307/520513, 1979.

Haeberli, W.: Investigating glacier-permafrost relationships in high-mountain areas: historical background, selected examples and research needs, Geological Society, London, Special Publications, 242, 29–37, https://doi.org/10.1144/GSL.SP.2005.242.01.03, 2005.

Haeberli, W. and Vonder Mühll, D. S.: On the characteristics and possible origins of ice in rock glacier permafrost, Zeitschrift für Geomorphologie, Supplementband, 104, 43–57, 1996.

Haeberli, W., Hallet, B., Arenson, L., Elconin, R., Humlum, O., Kääb, A., Kaufmann, V., Ladanyi, B., Matsuoka, N., Springman, S., and Mühll, D. V.: Permafrost creep and rock glacier dynamics, Permafrost Periglac. Process., 17, 189–214, https://doi.org/10.1002/ppp.561, 2006.

Haeberli, W., Arenson, L. U., Wee, J., Hauck, C., and Mölg, N.: Discriminating viscous-creep features (rock glaciers) in mountain permafrost from debris-covered glaciers – a commented test at the Gruben and Yerba Loca sites, Swiss Alps and Chilean Andes, The Cryosphere, 18, 1669–1683, https://doi.org/10.5194/tc-18-1669-2024, 2024.

Harris, C. and Murton, J. B.: Interactions between glaciers and permafrost: an introduction, SP, 242, 1–9, https://doi.org/10.1144/GSL.SP.2005.242.01.01, 2005.

Harris, S. A. and Pedersen, D. E.: Thermal regimes beneath coarse blocky materials, Permafrost and Periglacial Processes, 9, 107–120, 1998.

Hartmeyer, I. and Otto, J.-C.: Rockfall, glacier recession, and permafrost degradation: long-term monitoring of climate change impacts at the Open-Air-Lab Kitzsteinhorn, Hohe Tauern, DEUQUA Spec. Pub., 5, 3–12, https://doi.org/10.5194/deuquasp-5-3-2024, 2024.

Hauck, C.: New Concepts in Geophysical Surveying and Data Interpretation for Permafrost Terrain: Geophysical Surveying in Permafrost Terrain, Permafrost and Periglac. Process., 24, 131–137, https://doi.org/10.1002/ppp.1774, 2013.

Herring, T., Lewkowicz, A. G., Hauck, C., Hilbich, C., Mollaret, C., Oldenborger, G. A., Uhlemann, S., Farzamian, M., Calmels, F., and Scandroglio, R.: Best practices for using electrical resistivity tomography to investigate permafrost, Permafrost & Periglacial, 34, 494–512, https://doi.org/10.1002/ppp.2207, 2023.

Hilbich, C., Marescot, L., Hauck, C., Loke, M. H., and Mäusbacher, R.: Applicability of electrical resistivity tomography monitoring to coarse blocky and ice-rich permafrost landforms, Permafrost Periglac. Process., 20, 269–284, https://doi.org/10.1002/ppp.652, 2009.

Hu, Y., Arenson, L. U., Barboux, C., Bodin, X., Cicoira, A., Delaloye, R., Gärtner-Roer, I., Kääb, A., Kellerer-Pirklbauer, A., Lambiel, C., Liu, L., Pellet, C., Rouyet, L., Schoeneich, P., Seier, G., and Strozzi, T.: Rock Glacier Velocity: An Essential Climate Variable Quantity for Permafrost, Reviews of Geophysics, 63, e2024RG000847, https://doi.org/10.1029/2024RG000847, 2025.

Huss, M., Dhulst, L., and Bauder, A.: New long-term mass-balance series for the Swiss Alps, J. Glaciol., 61, 551–562, https://doi.org/10.3189/2015JoG15J015, 2015.

Kellerer-Pirklbauer, A., Bodin, X., Delaloye, R., Lambiel, C., Gärtner-Roer, I., Bonnefoy-Demongeot, M., Carturan, L., Damm, B., Eulenstein, J., Fischer, A., Hartl, L., Ikeda, A., Kaufmann, V., Krainer, K., Matsuoka, N., Morra Di Cella, U., Noetzli, J., Seppi, R., Scapozza, C., Schoeneich, P., Stocker-Waldhuber, M., Thibert, E., and Zumiani, M.: Acceleration and interannual variability of creep rates in mountain permafrost landforms (rock glacier velocities) in the European Alps in 1995–2022, Environ. Res. Lett., 19, 034022, https://doi.org/10.1088/1748-9326/ad25a4, 2024.

Kenner, R., Phillips, M., Beutel, J., Hiller, M., Limpach, P., Pointner, E., and Volken, M.: Factors Controlling Velocity Variations at Short-Term, Seasonal and Multiyear Time Scales, Ritigraben Rock Glacier, Western Swiss Alps, Permafrost & Periglacial, 28, 675–684, https://doi.org/10.1002/ppp.1953, 2017.

Kenner, R., Pruessner, L., Beutel, J., Limpach, P., and Phillips, M.: How rock glacier hydrology, deformation velocities and ground temperatures interact: Examples from the Swiss Alps, Permafrost & Periglacial, 31, 3–14, https://doi.org/10.1002/ppp.2023, 2020.

Kneisel, C.: Assessment of subsurface lithology in mountain environments using 2D resistivity imaging, Geomorphology, 80, 32–44, https://doi.org/10.1016/j.geomorph.2005.09.012, 2006.

Kneisel, C. and Kääb, A.: Mountain permafrost dynamics within a recently exposed glacier forefield inferred by a combined geomorphological, geophysical and photogrammetrical approach, Earth Surf. Process. Landforms, 32, 1797–1810, https://doi.org/10.1002/esp.1488, 2007.

Kneisel, C., Haeberli, W., and Baumhauer, R.: Comparison of spatial modelling and field evidence of glacier/permafrost relations in an Alpine permafrost environment, Ann. Glaciol., 31, 269–274, https://doi.org/10.3189/172756400781820093, 2000.

Kneisel, C., Hauck, C., Fortier, R., and Moorman, B.: Advances in geophysical methods for permafrost investigations, Permafrost Periglac. Process., 19, 157–178, https://doi.org/10.1002/ppp.616, 2008.

Kneisel, C.: Permafrost in recently deglaciated glacier forefields - measurements and observations in the eastern Swiss Alps and northern Sweden, zfg, 47, 289–305, https://doi.org/10.1127/zfg/47/2003/289, 2003.

Kunz, J. and Kneisel, C.: Glacier–Permafrost Interaction at a Thrust Moraine Complex in the Glacier Forefield Muragl, Swiss Alps, Geosciences, 10, 205, https://doi.org/10.3390/geosciences10060205, 2020.

Kunz, J., Ullmann, T., and Kneisel, C.: Internal structure and recent dynamics of a moraine complex in an alpine glacier forefield revealed by geophysical surveying and Sentinel-1 InSAR time series, Geomorphology, 398, 108052, https://doi.org/10.1016/j.geomorph.2021.108052, 2022.

Marcer, M., Serrano, C., Brenning, A., Bodin, X., Goetz, J., and Schoeneich, P.: Evaluating the destabilization susceptibility of active rock glaciers in the French Alps, The Cryosphere, 13, 141–155, https://doi.org/10.5194/tc-13-141-2019, 2019.

Marescot, L., Loke, M. H., Chapellier, D., Delaloye, R., Lambiel, C., and Reynard, E.: Assessing reliability of 2D resistivity imaging in mountain permafrost studies using the depth of investigation index method, Near Surface Geophysics, 1, 57–67, https://doi.org/10.3997/1873-0604.2002007, 2003.

MeteoSwiss: Mean precipitation 1991-2020, https://data.geo.admin.ch/browser/index.html#/collections/ch.meteoschweiz.klimanormwerte-niederschlag_aktuelle_periode/items/klimanormwerte-niederschlag_aktuelle_periode?.language=en (last access: 07.04.2025), 2023a.

MeteoSwiss: Mean temperature 1991-2020, https://data.geo.admin.ch/browser/index.html#/collections/ch.meteoschweiz.klimanormwerte-temperatur_aktuelle_periode/items/klimanormwerte-temperatur_aktuelle_periode?.language=en (last access: 07.04.2025), 2023b.

Noetzli, J., Isaksen, K., Barnett, J., Christiansen, H. H., Delaloye, R., Etzelmüller, B., Farinotti, D., Gallemann, T., Guglielmin, M., Hauck, C., Hilbich, C., Hoelzle, M., Lambiel, C., Magnin, F., Oliva, M., Paro, L., Pogliotti, P., Riedl, C., Schoeneich, P., Valt, M., Vieli, A., and Phillips, M.: Enhanced warming of European mountain permafrost in the early 21st century, Nat Commun, 15, 10508, https://doi.org/10.1038/s41467-024-54831-9, 2024.

Nyenhuis, M.: Permafrost und Sedimenthaushalt in einem alpinen Geosystem, Ph.D. thesis, Rheinische Friedrich–Wilhelms–Universität Bonn, Germany, 228 pp., 2005.

Otto, J.-C., Schrott, L., Jaboyedoff, M., and Dikau, R.: Quantifying sediment storage in a high alpine valley (Turtmanntal, Switzerland), Earth Surf Processes Landf, 34, 1726–1742, https://doi.org/10.1002/esp.1856, 2009.

Otto, J.-C.: Paraglacial sediment storage quantification in the Turtmann Valley, Swiss Alps, Ph.D. thesis, Rheinische Friedrich–Wilhelms–Universität Bonn, Germany, 2006.

Pfluger, F., Weber, S., Steinhauser, J., Zangerl, C., Fey, C., Fürst, J., and Krautblatter, M.: Massive permafrost rock slide under a warming polythermal glacier deciphered through mechanical modeling (Bliggspitze, Austria), Earth Surf. Dynam., 13, 41–70, https://doi.org/10.5194/esurf-13-41-2025, 2025.

Rock glacier inventories and kinematics (RGIK): Guidelines for inventorying rock glaciers: Baseline and practical concepts (Version 1.0), IPA Action Group Rock glacier inventories and kinematics, https://doi.org/10.51363/unifr.srr.2023.002, 2023.

Rödder, T. and Kneisel, C.: Influence of snow cover and grain size on the ground thermal regime in the discontinuous permafrost zone, Swiss Alps, Geomorphology, 175–176, 176–189, https://doi.org/10.1016/j.geomorph.2012.07.008, 2012a.

Rödder, T. and Kneisel, C.: Permafrost mapping using quasi-3D resistivity imaging, Murtèl, Swiss Alps, Near Surface Geophysics, 10, 117–127, https://doi.org/10.3997/1873-0604.2011029, 2012b.

https://doi.org/10.5194/egusphere-2025-1671
Preprint. Discussion started: 15 May 2025


Rouyet, L., Lauknes, T. R., Christiansen, H. H., Strand, S. M., and Larsen, Y.: Seasonal dynamics of a permafrost landscape, Adventdalen, Svalbard, investigated by InSAR, Remote Sensing of Environment, 231, 111236, https://doi.org/10.1016/j.rse.2019.111236, 2019.

Rücker, C., Günther, T., and Spitzer, K.: Three-dimensional modelling and inversion of dc resistivity data incorporating topography - I. Modelling, Geophysical Journal International, 166, 495–505, https://doi.org/10.1111/j.1365-246X.2006.03010.x, 2006.

Sandwell, D. T. and Price, E. J.: Phase gradient approach to stacking interferograms, J. Geophys. Res., 103, 30183–30204, https://doi.org/10.1029/1998JB900008, 1998.

Scherler, M., Schneider, S., Hoelzle, M., and Hauck, C.: A two-sided approach to estimate heat transfer processes within the active layer of the Murtèl–Corvatsch rock glacier, Earth Surf. Dynam., 2, 141–154, https://doi.org/10.5194/esurf-2-141-2014, 2014.

Sommer, C., Malz, P., Seehaus, T. C., Lippl, S., Zemp, M., and Braun, M. H.: Rapid glacier retreat and downwasting throughout the European Alps in the early 21st century, Nat Commun, 11, 3209, https://doi.org/10.1038/s41467-020-16818-0, 2020.

Streletskiy, D., Noetzli, J., Smith, S. L., Vieira, G., Schoeneich, P., Hrbacek, F., and Irrgang, A. M.: Strategy and Implementation Plan for the Global Terrestrial Network for Permafrost (GTN-P) 2021-2024, https://doi.org/10.5281/ZENODO.6075468, 31 December 2021.

Strozzi, T., Caduff, R., Jones, N., Barboux, C., Delaloye, R., Bodin, X., Kääb, A., Mätzler, E., and Schrott, L.: Monitoring Rock Glacier Kinematics with Satellite Synthetic Aperture Radar, Remote Sensing, 12, 559, https://doi.org/10.3390/rs12030559, 2020.

Tatenhove, F. V. and Dikau, R.: Past and Present Permafrost Distribution in the Turtmanntal, Wallis, Swiss Alps, Arctic and Alpine Research, 22, 302–316, https://doi.org/10.1080/00040851.1990.12002794, 1990.

Villarroel, C. D., Ortiz, D. A., Forte, A. P., Tamburini Beliveau, G., Ponce, D., Imhof, A., and López, A.: Internal structure of a large, complex rock glacier and its significance in hydrological and dynamic behavior: A case study in the semi-arid Andes of Argentina, Permafrost & Periglacial, 33, 78–95, https://doi.org/10.1002/ppp.2132, 2022.

Vincent, C., Fischer, A., Mayer, C., Bauder, A., Galos, S. P., Funk, M., Thibert, E., Six, D., Braun, L., and Huss, M.: Common climatic signal from glaciers in the European Alps over the last 50 years, Geophysical Research Letters, 44, 1376–1383, https://doi.org/10.1002/2016GL072094, 2017.

Vivero, S., Hendrickx, H., Frankl, A., Delaloye, R., and Lambiel, C.: Kinematics and geomorphological changes of a destabilising rock glacier captured from close-range sensing techniques (Tsarmine rock glacier, Western Swiss Alps), Front. Earth Sci., 10, 1017949, https://doi.org/10.3389/feart.2022.1017949, 2022.

Vonder Mühll, D.: Geophysikalische Untersuchungen im Permafrost des Oberengadins, Ph.D. thesis, ETH Zurich, Switzerland, https://doi.org/10.3929/ETHZ-A-000891391, 1993.

Waller, R. I.: Glacier-permafrost interactions, Wiley, Hoboken, NJ, 306 pp., ISBN  978-1-118-62098-4, 2024.

Waller, R. I., Murton, J. B., and Kristensen, L.: Glacier–permafrost interactions: Processes, products and glaciological implications, Sedimentary Geology, 255–256, 1–28, https://doi.org/10.1016/j.sedgeo.2012.02.005, 2012.

Wee, J. and Delaloye, R.: Post-glacial dynamics of an alpine Little Ice Age glacitectonized frozen landform (Aget, western Swiss Alps), Permafrost & Periglacial, 33, 370–385, https://doi.org/10.1002/ppp.2158, 2022.

Wee, J., Vivero, S., Mathys, T., Mollaret, C., Hauck, C., Lambiel, C., Beutel, J., and Haeberli, W.: Characterizing ground ice content and origin to better understand the seasonal surface dynamics of the Gruben rock glacier and the adjacent Gruben debris-covered glacier (southern Swiss Alps), https://doi.org/10.5194/egusphere-2024-1283, 8 May 2024.

Wirz, V., Gruber, S., Purves, R. S., Beutel, J., Gärtner-Roer, I., Gubler, S., and Vieli, A.: Short-term velocity variations at three rock glaciers and their relationship with meteorological conditions, Earth Surf. Dynam., 4, 103–123, https://doi.org/10.5194/esurf-4-103-2016, 2016.

World Meteorological Organization (WMO) (Ed.): The 2022 GCOS ECVs Requirements, Geneva, 2022.